

MODELLING OF BEAM PARAMETERS OF RF LINAC FOR GBS-ELI-NP

Piotr Tracz[†]

for the ELI-NP team

ELI-NP/IFIN-HH, RO-077125 Bucharest-Magurele, Romania

Abstract

The Gamma Beam System at the ELI-NP (Extreme Light Infrastructure – Nuclear Physics) currently being constructed in Magurele/Bucharest, Romania will be a high-brilliance advanced source of gamma rays based on laser Compton back-scattering. For a successful operation of the GBS a high brightness low emittance electron beam is of crucial importance. The warm RF linac is designed in two stages – one with the beam up to 300 MeV, and another one about 720 MeV. The S-band photo-injector is combined with a C-band linac. The beam is transported by transfer lines to the interaction points. In this paper we report the results of computer simulations of the electron beam transport in the low energy linac and transfer line up to the low energy interaction point (IP1). The simulation model makes it possible to predict the beam parameters to be recuperated in case of failure of any magnetic or accelerating elements as well as it enables to determine the optimal parameters of replaced components. It will be used for the development of the Gamma Beam System in the future.

INTRODUCTION

The Gamma Beam System was designed and is being constructed by the EuroGammaS Association – a consortium of European academic and research institutions and industrial partners, and it is hosted by the Horia Hulubei National Institute of Physics and Nuclear Engineering [1]. The technical design of GBS is described with details in [2], and several other publications like e.g. [3-5].

To perform the simulations we used the Elegant [6] code, and SDDS toolkit [7] for processing and graphing of the Elegant output data. The simulations of the beam transport in the injector and calculations of output beam parameters at the injector exit were done with use of the program Parmela [8, 9]. Currently we are studying beam optimization in the injector using the Astra [10] code.

Our study will be extended for the high energy linac. The aim is to provide means to re-optimize the linac settings to new working points in accordance to users' requirements.

S-band Injector

The GBS injector starts at the RF gun with photo-cathode. To suppress the beam loss by transverse spreading there are two focusing solenoid magnets with high gradient field starting very close to the gun exit. They focus the beam to minimum size and make the beam emittance low at the entrance of accelerating structure. The photo-cathode RF gun generates electron beam in the

photoemission process. Ultraviolet laser pulses are incident on the copper photo cathode. The charge of the electron bunches depends on the laser power and the conversion efficiency of the photo-cathode material; in case of GBS it is 250pC. The 2D profile of the gun with electric field pattern designed in the electromagnetic code Superfish [11] is shown in Fig. 1. It will operate at π -mode with resonance frequency 2.856GHz with an input power sufficient to achieve 120MeV/m field gradient at cathode.

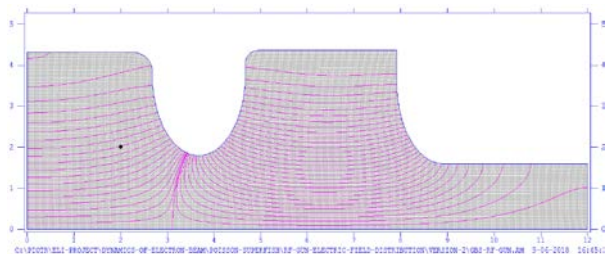


Figure 1: 2D profile of RF gun for GBS with electric field profile.

The RF gun is followed by two TW accelerating structures. These are constant gradient (22MV/m), and will operate in $2\pi/3$ mode. The first structure is surrounded by twelve independent coils. The purpose of them is to keep the radius of the beam from the entrance along the accelerating sections. Additionally the S-band sections will act as a bunch compressor.

Low Energy C-band Linac

The low energy linac that follows the injector is based on four C-band sections operating at 5.712 GHz. The length of each section is 1.78449m and the length of a single cell is 0.017495m. Each section is fed by 52MV RF voltage. The input RF phase of the first two sections is 82.5° and other two 115° . The dogleg type transport line transmits the beam to the interaction point. After the interaction point the beam is transported to the beam dump.

In addition to the accelerating sections the linac modules are completed by magnetic and diagnostic devices. There are two quadrupole triplets in the diagnostic sections. One after the first C-band structure and another one at the end of the low energy linac. They are used for emittance measurement and to provide the desired electron beam focusing. There are several beam profile monitors (screens) located at different positions along the linac to control the transverse profile of the beam. Figure 2 presents the distribution of the quadrupole magnets and the profile monitors in the low energy linac. Two S-band transverse deflecting structures will be used for measuring the longitudinal beam profile.

[†] email address: piotr.tracz@eli-np.ro

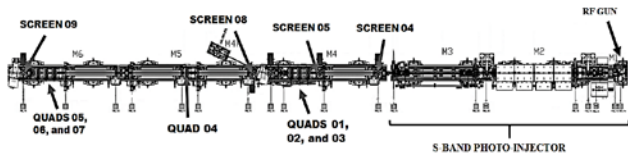


Figure 2: Location of quadrupole magnets and profile monitors in the low energy linac [2].

Transfer Line

The transfer line starts at the dipole magnet. There are two quadrupole triplets. The dispersion of the beam after dipole magnet 01 is corrected by dipole 02. Figure 3 shows the components of the transfer line.

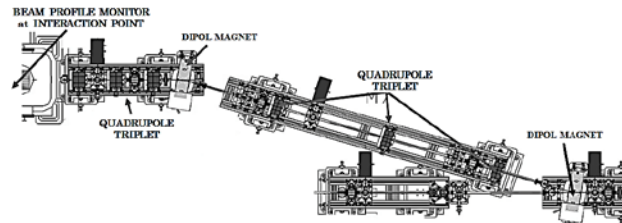


Figure 3: Location of quadrupole magnets and profile monitors in transfer line [2].

RESULTS

Elegant Simulations

For the simulations with the Elegant code 50 000 particles were used. The beam charge $Q = 250\text{pC}$, output beam energy at the injector exit $E = 81\text{MeV}$, bunch length $\sigma_z \approx 280\mu\text{m}$, the transverse normalized emittance (1σ) at the injector exit (screen 04), calculated from the Elegant output data is $\varepsilon_{n,x,y} \approx 0.43 [\mu\text{m} \cdot \text{rad}]$. Input Twiss parameters [9] are: $\beta_x = 31.69$, $\alpha_x = -1.98$, $\eta_x = 0$, $\beta_y = 31.71$, $\alpha_y = -1.99$, $\eta_y = 0$.

Figure 4 below presents the evolution of the transverse beam profile along the low energy linac, and transfer line.

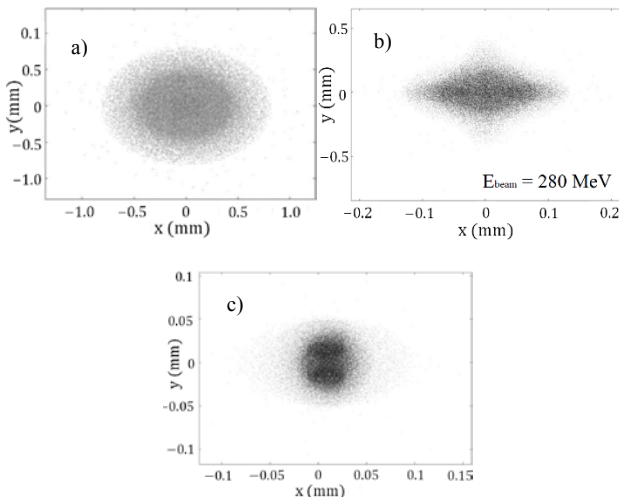


Figure 4: Transverse beam profiles at: injector exit (a), end of low energy linac (b), and interaction point IP1 (c).

The transverse (Figure 5) and longitudinal (Figure 6) beam distributions are the histograms of three coordinates x, y, z . The z coordinate is calculated from the relationship $z = \beta ct$, where βc is the velocity of the particle, and t is time of arrival at the observation point. Figures below include the *rms* sizes of the bunch.

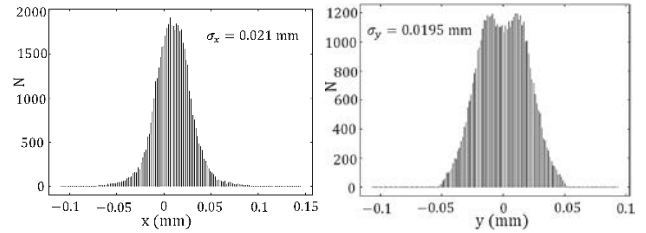


Figure 5: Transverse beam distribution at IP1.

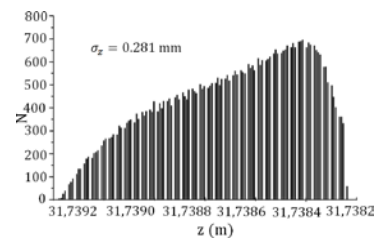


Figure 6: Longitudinal beam distribution at IP1.

A good approximation for the beam shape in phase space is elliptic. An ellipse can be defined by specifying: area, shape, and orientation. The *beta* function $\beta(s)$ is related to the beam shape and size. The beam envelope is determined by the beam emittance and the function $\beta(s)$. The *beta* function is highly dependent on the particular arrangement of the quadrupole magnets. The *alpha* function $\alpha(s)$ is related to the tilt (i.e. orientation) of the beam ellipse. Figures 7 and 8 depict the functions $\beta(s)$ and $\alpha(s)$ along the low energy linac and the transfer line up to IP1. The *gamma* function depends on α - and β -functions in accordance to the relation $\gamma(s) = \frac{1+\alpha^2(s)}{\beta(s)}$.

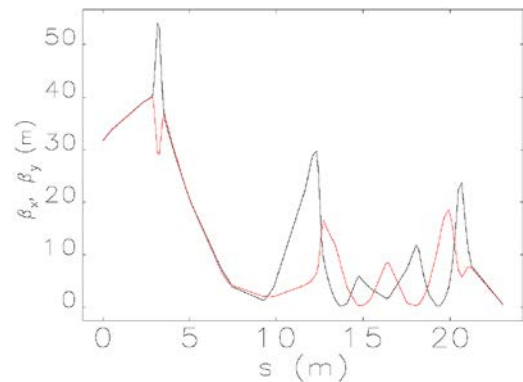


Figure 7: Function *beta* from photo-injector exit down to low energy interaction point IP1 (β_x -black line, β_y -red line).

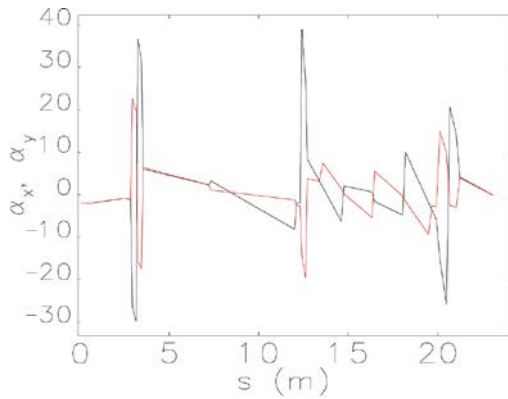


Figure 8: Function α from photo-injector exit down to low energy interaction point IP1 (α_x -black line, α_y -red line).

The normalized emittance (1σ) at the IP1 calculated from the Elegant output data is $\epsilon_{n,x,y} = 0.43\text{-}0.45$ [$\mu\text{m} \cdot \text{rad}$].

In Fig. 9 the transverse phase space at IP1 is given.

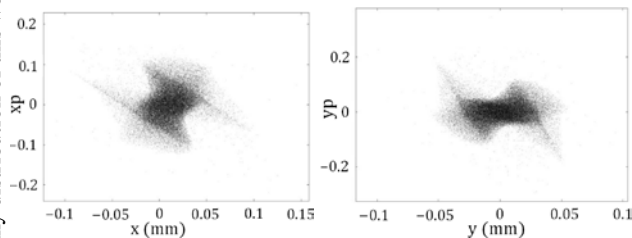


Figure 9: Transverse (horizontal – left, vertical - right) phase space at IP1.

Figure 10 presents the beam energy spread and beam energy at IP1, and Fig. 11 the energy distribution along the bunch.

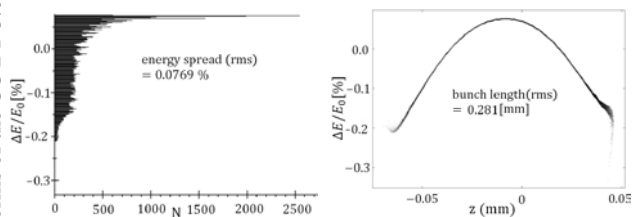


Figure 10: Beam energy spread (left) and energy distribution (right) at IP1.

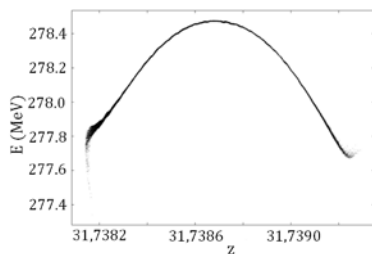


Figure 11: Energy distribution along bunch at IP1.

CONCLUSIONS

We presented the results obtained in simulating the beam transport in the low energy linac and the transfer line for the ELI-NP Gamma Beam System. We used the Elegant code. Our study will be extended for the high energy linac. Calculations of the injector will also be done with use of the Astra code.

ACKNOWLEDGEMENTS

The GBS-ELI-NP project is co-funded by the European Union through the European Regional Development Fund.

REFERENCES

- [1] <http://www.nipne.ro/> and <http://www.eli-np.ro/>
- [2] O. Adriani et al., “Technical Design Report; EuroGammaS proposal for the ELI-NP Gamma Beam System”, arXiv: 1407.3669v1 [physics.acc-ph].
- [3] A. Bacci et al., “Electron linac design to drive bright Compton back-scattering gamma-ray sources”, J. Appl. Phys. vol. 113, p. 194508, 2013, doi:10.1063/1.4805071
- [4] C. Vaccarezza et al., “Optimization studies for the beam dynamic in the RF linac of the ELI-NP gamma beam system”, in Proc. IPAC2016, Busan, Korea, May 2016, paper TUPOW041, pp. 1850-1853.
- [5] P. Tracz, “ELI-NP gamma beam system – new facility for nuclear physics research”, in Proc. PPC2017, Brighton, Great Britain, Jun. 2017, pp. 1-4, doi:10.1109/PPC.2017.8291290
- [6] M. Borland, “Elegant: A flexible SDDS-compliant code for accelerator simulation”, Advanced Photon Source LS-287, September 2000.
- [7] M. Borland, <https://ops.aps.anl.gov/SDDSIntroTalk/slides.html>
- [8] L.M. Young, “PARMELA”, Los Alamos National Laboratory Report LA-UR-96-1835 (1996).
- [9] C. Vaccarezza, private communication.
- [10] ASTRA, K. Floettmann <http://www.desy.de/~mpyflo/>
- [11] laacg.lanl.gov/laacg/services/download_sf.shtml

Content from this work may be used under the terms of the CC BY 3.0 licence (© 2018). Any distribution of this work must maintain attribution to the author(s), title of the work, publisher, and DOI.